Impact of dust deposition on the albedo of Vatnajökull ice cap, Iceland.

Monika Wittmann [1], Christine D. Groot Zwaaftink [2], Louise Steffensen Schmidt [1] , Sverrir
Guðmundsson [1,3], Finnur Pálsson [1], Olafur Arnalds [4], Helgi Björnsson [1], Throstur Thorsteinsson [1],
Andreas Stohl [2]

[1] Institute of Earth Sciences, University of Iceland, Reykjavik, Iceland; [2] NILU - Norwegian Institute for
Air Research, Kjeller, Norway, [3] Keilir, Institute of Technology, Reykjanesbær, Iceland; [4] Agricultural
University of Iceland, Hvanneyri, Iceland

Correspondence to: Monika Wittmann (mod3@hi.is)

Abstract

Deposition of small amounts of airborne dust on glaciers causes positive radiative forcing and
enhanced melting due to the reduction of surface albedo. To study the effects of dust deposition on
the mass balance of Brúarjökull, an outlet glacier of the largest ice cap in Iceland, Vatnajökull, a study
of dust deposition events in the year 2012 was carried out. The dust-mobilization module FLEXDUST
was used to calculate spatiotemporally resolved dust emissions from Iceland and the dispersion
model FLEXPART was used to simulate atmospheric dust dispersion and deposition. We used albedo
measurements at two automatic weather stations on Brúarjökull to evaluate the dust impacts. Both
stations are situated in the accumulation area of the glacier, but the lower station is close to the
equilibrium line. For this site (~1210 m a.s.l.), the dispersion model produced 10 major dust
deposition events and a total annual deposition of 20.5 g m^{-2}. At the station located higher on the
glacier (~1525 m a.s.l.), the model produced nine dust events, with one single event causing ~5 g m^{-2}
dust deposition and a total deposition of ~10 g m^{-2} yr^{-1}. The main dust source was found to be the
Dyngjusandur floodplain north of Vatnajökull; northerly winds prevailed 80% of the time at the lower
station when dust events occurred. In all of the simulated dust events, a corresponding albedo drop
was observed at the weather stations. The influence of the dust on the albedo was estimated by
using the regional climate model HIRHAM5 to simulate the albedo of a clean glacier surface without
dust. By comparing the measured albedo to the modelled albedo, we determine the influence of
dust events on the snow albedo and the surface energy balance. We estimate that the dust
deposition caused an additional 1.1 m w.e. (water equivalent) of snow melt (or 42% of the 2.8 m w.e.
total melt) compared to a hypothetical clean glacier surface at the lower station, and 0.6 m w.e.
more melt (or 38% of the 1.6 m w e. melt in total) at the station located further upglacier. Our
findings show that dust has a strong influence on the mass balance of glaciers in Iceland.

Key words: dust events, glacier, energy balance, snow melt, surface melt, FLEXPART, albedo

1. Introduction

35   The cryosphere is an important part of the global climate system. Small changes in reflected and absorbed radiation at snow or ice surfaces can have large impacts on the state of the cryosphere, and on Earth's climate and its hydrological cycle (e.g., Budyko, 1969, Flanner et al., 2007, Painter et al., 2013). Albedo, the reflectivity of a surface, is a dominant component of the surface energy balance. The albedo of snow depends e.g. on the snow grain size, wetness and impurities in the near-

40   surface snow layer (e.g. Wiscombe and Warren, 1980; Meinander et al., 2014). Estimation of snow albedo is important to predict seasonal snowmelt and runoff rates and for calculating the regional and global energy budget. Due to impurities in snow, the albedo of the snow can be reduced. This involves direct albedo reduction by the impurities but also changes in the snow grain size triggered by the impurities especially at temperatures close to the melting point, which can strongly enhance

45   the albedo reduction (Hansen and Nazarenko, 2004; Myhre et al., 2013). Melting of the snow can further reduce the albedo if underlying ground with much lower albedo is exposed. This initiates a positive feedback loop, i.e. more snow melt results in more absorbed radiation which in turn amplifies the melting. Even though direct global radiative forcing of mineral dust in the atmosphere is calculated as negative in the IPCC report (IPCC, 2013), regionally this depends on both the optical

50   properties of the dust, deposited amounts and the albedo of the underlying surface. Icelandic volcanic dust (mostly from basaltic material) is darker and more absorbing than mineral dust from most other regions. It is expected to cause positive radiative forcing, due to its dark colour, the high albedo of snow and ice, and a *clumping mechanism*, where fine dust impurities in snow form larger particles (Dagsson-Waldhauserova et al., 2015) and accelerate snow melt. In this study, the term

55   *radiative forcing* means the instantaneous surface enhanced absorption due to deposited dust (Painter et al., 2007). In its effect on snow albedo, dust is somewhat similar to black carbon (Yoshida et al., 2016; Goelles et al., 2015) which has received much interest recently as a short-lived climate forcer, especially in the Arctic (e.g. Quinn et al., 2008; AMAP, 2015; Meinander et al., 2016). Other studies (e.g. Di Mauro et al., 2015 , Zhao et al., 2014, He et al., 2014), have shown the impact of dust

60   and black carbon and their effect on radiative forcing and energy balance.

Painter et al. (2007) have shown that snow cover duration in a mountain range in the United States was shortened through surface shortwave radiative forcing by deposition of desert dust. Similarly, Flanner et al. (2014) have shown that the snow albedo effect of deposited volcanic ash from an eruption in Iceland could counteract the otherwise negative radiative forcing of volcanic eruptions

65   caused by sulphur emissions. Increased snow impurity content has an important effect on the albedo

of the Greenland Ice sheet. Dumont et al. (2014) estimated that the contribution by impurities to surface mass balance was at least -27 Gt^{-1} in recent years. A positive feedback loop is created because impurities mostly concentrate on the surface, lowering the albedo and amplify surface melt. Seasonal snow cover duration is expected to be shortened which then can further increase the amount of dust transported to the ice sheet and intensify the decrease in albedo (Doherty et al., 2013, Dumont et al., 2014). This will lead to an increased impact of climate change on mass balance and corresponding sea level rise of the Greenland ice sheet compared to current predictions ignoring this effect (Dumont et al., 2014).

Recent modelling studies have shown that transport of dust from Iceland is a substantial dust source for Greenland (Groot Zwaaftink et al., 2016; Baddock et al., 2017). Furthermore, volcanic eruptions such as in 2010 and 2011 can have a large impact (Petit et al., 2013; Davies et al., 2010).

Sources of dust in Iceland are the proglacial areas and sandy deserts which cover more than 22% of Iceland (Arnalds et al., 2001). Even though Iceland is not situated in an arid climate, it's aeolian activity is very high (Arnalds et al., 2016), due to the large area of sandur plains and frequent strong winds resulting in numerous dust events. On average, 135 dust days per year occurred in Iceland, with 101 dust days in south Iceland and 34 dust days in northeast Iceland including dust haze and resuspension of volcanic material, where a *dust day* is defined as a day when at least one weather station recorded at least one dust observation (Dagsson-Waldhauserova et al., 2013, 2014). Airborne redistribution of dust has a strong influence on climate, snowmelt and Icelandic soils. Satellite images have shown that dust particles can be transported over the Atlantic and Arctic Ocean, sometimes for more than 1000 km (Arnalds, 2010; Baddock et al., 2017). Therefore, Icelandic dust is likely to contribute to Arctic and European air pollution and can affect the climate via dust deposition on Arctic glaciers or sea ice (Arnalds et al., 2016). Icelandic glaciers cover about 11% of the country and the focus area of this study is Vatnajökull, Iceland's largest glacier with an area of more than 8000 km^2 (Figure 1) and the largest ice cap in Europe outside the polar regions (Björnsson and Pálsson, 2008). In the year 2000 the area of the ice cap was ~8100 km^2 with a volume of ~3100 km^3. If all of this ice would melt, this would lead to a global sea level rise by ~1cm. The average ice thickness is 380 m, with a maximum thickness of about 950 m. The elevation of the ice cap ranges from sea level up to 2110 m a.s.l. (Björnsson and Pálsson 2008, Björnsson et al. 2013). Mass balance has been surveyed since 1991/92, with a typical mass balance of ~1.5 m w.e. The annul balance was positive the first years measured, but negative after 1995 (Björnsson et al. 2013), with the exception of 2014/15; the average mass balance after 1995 is -0,65 m w.e.

In this study we explore what impact dust events in Iceland have on the glacier surface albedo, how often they occur and what their impact on the energy balance of glaciers in Iceland is. Therefore,

100   dust deposition rates were calculated with a dispersion model and compared with albedo measurements on an Icelandic glacier.

2. Methods

2.1. Dust transport modelling

A recently developed scheme for dust mobilization, called FLEXDUST (Groot Zwaaftink et al., 2016) is
105   used to estimate dust emission. The model can be applied globally, but in this study we only included dust emission from Icelandic sources. FLEXDUST produces dust emission estimates that can be imported directly into the Lagrangian particle dispersion model FLEXPART (Stohl et al., 1998, 2005) to estimate mineral dust transport, concentrations in the atmosphere and deposition on global and regional scales. FLEXDUST is based on meteorological data from the European Centre for Medium-
110   Range Weather Forecasts (ECMWF), land cover data by the Global Land Cover by National Mapping Organizations (GLCNMO) and additionally, for Iceland, a high-resolution (~1 arcsec) land cover data set that identifies sandy deserts is used (Dagsson-Waldhauserova et al., 2014; Arnalds, 2015). In FLEXDUST, dust can be emitted in regions where mineral dust is available according to the land cover data set. If snow cover exceeds a thickness of 10 cm, dust emission is inhibited. Dust emission is
115   initiated in regions with erodible materials if a threshold friction velocity is exceeded. Contrary to the standard version of FLEXDUST, for this study dust mobilization was assumed not to be influenced by soil moisture. The dust source regions in Iceland are more sediment-like than actual soils and the correct functioning of the soil moisture model is questionable for these sources, which often dry out very quickly at the surface after a precipitation event (Dagsson-Waldhauserova et al., 2014). This may
120   enable dust mobilization shortly after a precipitation event. The exclusion of dust emission during precipitation is better describing the process of surface wetting. Therefore, in this version of FLEXDUST, dust emission is inhibited in case of precipitation but does not depend on soil moisture. We further used a combination of the erosion classes described by Arnalds et al. (2010) and the threshold values observed by Arnalds et al. (2001) to estimate threshold friction velocity. Once
125   mobilization thresholds are exceeded, dust emission rates are calculated following Marticorena and Bergametti (1995). It is assumed that emitted dust particles have a size between 0.2 and 18.2 µm and follow a size distribution after Kok (2011). Dust emission rates were calculated on a grid with 0.1˚x0.1˚ resolution for Iceland, and with a time resolution of 3 hours.

Using the dust emission rates provided by FLEXDUST, dispersion of the dust in the atmosphere was
130   simulated with FLEXPART version 10. Our simulations were driven with ECMWF operational analysis data with a resolution of 1˚x1˚ globally and a nest over Iceland with 0.2˚x0.2˚ resolution. FLEXPART simulates dispersion by transporting particles using both resolved winds and stochastic motions

representing turbulence. Dust was carried in 10 size classes and was subject to both wet and dry removal. Further details about dust simulations with FLEXPART are provided by Groot Zwaaftink et al.

135   (2016). In the current study, dust concentrations and depositions during so-called dust events, i.e., events with strong dust deposition on Vatnajökull simulated by FLEXPART, were analysed. A minimum modelled concentration of 6 µg m^{-3} over at least two days was defined as dust event. In particular, we studied simulated dust events at two automatic weather stations (AWS) situated on Brúarjökull outlet (NE Vatnajökull, Figure 1), namely station B13 at ~1210 m a.s.l. and station B16 at

140   ~1525 m a.s.l.

2.2. Measurements

2012 was an extremely warm year in the northern hemisphere. For example, in Greenland new records were set for the total glacier mass loss, surface melt extent and duration (Tedesco et al., 2013; Nghiem et al., 2012, Dumont et al., 2014). Also in Iceland, 2012 was characterized by warm

145   temperatures, exceptionally low glacier albedo on Brúarjökull and negative glacier mass balances. Additionally, a significant number of northerly winds, likely transporting dust from Dyngjusandur towards Brúarjökull was observed. Furthermore, no volcanic eruptions that could complicate dust deposition and albedo analysis occurred in 2012. We therefore chose this year for analysis of dust events, albedo changes, glacier energy and mass balance. Besides this time series analysis in 2012,

150   we also modelled spatial distribution of dust deposition in 2013 and will compare model results to dust amounts in snow samples from October 7 2013. Unfortunately, such samples were not taken in 2012, but the comparison gives valuable insight in the spatial distribution that cannot be retrieved from the time series analysis. Time series of observed albedo and modelled dust deposition agreed better in 2012 than 2013.

155   Since 1996, AWS B13 and B16 at Brúarjökull have been used to measure the incoming (Q_i) and outgoing (Q_o) solar radiation, incoming (I_i) and outgoing (I_o) longwave radiation, wind direction, wind speed, air temperature and relative humidity at 2 m elevation above the surface (Guðmundsson et al., 2006). Albedo is estimated from measured incoming and reflected short wave radiation as $\alpha = Q_o/Q_i$. Daily albedo values were calculated as the average over 10 minute data obtained

160   between 13 and 14 UTC, when the solar zenith angle is smallest.

The AWS data, specifically albedo, temperature and wind, were compared with dust concentration and deposition values from FLEXPART for the measurement period in the year 2012 between days of the year (DOY) 130 and 283.

Surface snow samples, from the previous year's melted out firn layer, were collected on October 7

165   2013 at 16 sites on Vatnajökull (Dragosics et al. 2016). The samples contain dust deposited at these

sites during the summer of 2013. The top ~8 cm of snow including impurities were brought to the laboratory, where they were melted, evaporated and the mass of the dust was weighed. Additionally, two ~8 m long firn cores including dust layers from Brúarjökull (NE Vatnajökull), were drilled at B15 in 2015. The dust layers in the cores were dated depending on their depth and compared with mass balance measurements ($h_w \times \rho_w = h_f \times \rho_f$; where h_w is mass balance given as thickness of water, ρ_w is the density of water, h_f is the thickness of a firn layer and ρ_f is the density of firn). Dust deposition rates were estimated by measuring the mass of the dust content in the annual layers, and compared to model results (Table 1).

2.3. Surface energy balance calculations

The total energy balance (M) for a melting glacier surface is expressed as

$$M = R + H + Hp, \tag{1}$$

where $R = Q_i(1 - \alpha) + I_i - I_o$ is the net radiation obtained from the observed shortwave and longwave radiation components, and $H = H_d + H_l$ is the net turbulent flux of sensible (H_d) and latent (H_l) heat calculated from the observed temperature, humidity and wind speed within the boundary layer. A one-level model with stability factor and different roughness lengths for wind-speed, temperature and humidity, described in Guðmundsson et al. (2009) was used to calculate H_d and H_l. Heat supplied by precipitation (H_p) is considered negligible and the melt (ablation) m is calculated as

$$m = \begin{cases} \frac{M}{\rho_w \, L_f}; & M \geq 0 \\ 0; & M < 0 \end{cases} \tag{2}$$

where L_f is the latent heat of fusion (L_f = 3.34 10^5 J kg^{-1}) and ρ_w the density of water (1000 kg m^{-3}) (e.g. Guðmundsson et al., 2006).

Albedo is a key variable in the surface energy balance and it is used to calculate ice melting. If the energy balance is positive, this indicates an energy gain to the surface; if it is negative, it means an energy loss. The accuracy of the instruments (Kipp & Zonen CNR1, 2000) measuring longwave and shortwave radiation fluxes at AWSs was 3% (Guðmundsson et al., 2009).

To quantify the enhanced melt rates due to dust on the surface, the development of surface albedo for a dust free surface must be estimated at specific locations and meteorological conditions. This albedo estimate and in situ AWS data are used to calculate the energy balance at the AWS sites. The results can be compared to energy balance calculated from only the AWS data including the observed albedo. The development of surface albedo of snow is depending on meteorological

processes in the surface boundary layer, the energy budget of the surface, snowfall events etc. A regional climate model, which is forced with reanalysis data from a general circulation model at the lateral boundary and simulates the boundary layer meteorology and surface energy balance, can be used to simulate the clean surface albedo. Here we use the HIRHAM5 climate model. The HIRHAM5 model combines the dynamical core of the HIRLAM7 numerical forecasting model (Eerola, 2006) with the physical schemes from the ECHAM5 general circulation model (Roeckner et al., 2003). Model simulations have been validated over Greenland using AWS and ice core data (e.g. Lucas-Picher et al., 2012; Langen et al., 2015). Using the same method described in Langen et al. (2015), we run the surface scheme in HIRHAM5 by forcing it with atmospheric parameters from a previous model run. This method allows us to implement an improved albedo scheme (Nielsen-Englyst, 2015) without running the full model. This is described in more detail in the appendix and Schmidt et al. (submitted).

2.3.1.Evaluation of modelled albedo by HIRHAM5

As there was no ice at the surface at either of the two AWS's, we allowed the modelled clean surface albedo to drop to the value of clean firn, which we assumed to be 0.55. This value is based on the recommended value by Cuffey and Paterson (2010), but also represented in observed albedo in the years 2002, 2009 and 2014 (Appendix Fig. A1). For those years, measured albedo remained mostly above 0.55 for the whole measuring period. Under dry conditions the modelled albedo can only drop to 0.77. The albedo of fresh snow was assumed to be 0.9. Based on albedo measurements this value is assumed to be realistic after new snow events as seen in Fig. A1 in the Appendix. Sometimes measured albedo values especially in autumn can reach high values, even above 1. This can be explained due to the high solar zenith angle, multiple reflections and instrumental error (Kipp & Zonen CNR1, 2000).

The time scale τ_m, which determines how fast the albedo reaches its minimum value, was chosen to be 4 days, as it gives the best fit with the measurements without dropping below the measured values. In addition, this value gave the best fit when comparing with albedo measurements for other years with higher albedo (Appendix, Fig. A1 and Fig. A2), where the rate of the albedo decrease after a snow fall was realistic. Measured albedo might drop faster after a new snow event than predicted by the HIRHAM5 model because methamorphosis of fresh snow is fast at relatively high air temperatures (Oerlemans, 2001); light can also penetrate through a thin new snow layer, in which case the albedo also depends on the properties of the underlying snow layer (Wiscombe and Warren 1980), which may also contain dust.

The AWS B16 is situated in the accumulation area, but B13 is close to the equilibrium line of the glacier. This means that only in some years, as e.g. in 1997, 2004, 2005 and 2012 (Appendix Fig. A3) the mass balance was negative and the previous years' surface melted out at B13 and exposed firn with dust. Since 2012 was a year of very warm temperatures and negative mass balance, not only deposition during dust events influenced the albedo and energy balance. Warm and dry periods with northerly winds also increased the frequency of dust events. Due to the negative mass balance the exposed darker firn layer lowered the albedo additionally to surface dust. At station B13 between days 206 and 225 simulation values have been manually set to the minimum value of 0.55 because HIRHAM5 simulated a snowfall event, which was not observed.

3. Results

3.1. Spatial distribution of dust deposition 2013 and total deposition rates 2012 and 2013

The annual dust deposition distribution for the surface of Vatnajökull for 2013 showed a similar pattern in the model simulation and in the observations (Figure 2). The model simulated the highest concentrations in the south western part of Vatnajökull (Tungnaárjökull, Skaftárjökull, Síðujökull), followed by the north western and northern parts (Brúarjökull). This distribution is due to the major dust mobilization areas around Vatnajökull, such as Dyngjusandur, Tungná- and Skaftáöræfi (the area with severe erosion SW of Vatnajökull (Figure 1)), as well as the prevailing winds. The measurements of Dragosics et al. (2016) are shown as circles superimposed upon the modelled dust distribution in Figure 2. The average dust deposition for the 16 measurement locations was 2 g m^{-2}. The standard deviation of the measurements, 4 g m^{-2}, was quite high due to one outlier with a deposition value of 16.6 g m^{-2} in the SW on Tungnaárjökull. The average modelled deposition for the same locations as in the measurements is 6 g m^{-2}, with a standard deviation of 1 g m^{-2}. Thus, the model overestimated measured dust deposition by a factor of three and generated smaller dust variability. The latter was not surprising, given the relatively coarse resolution of the model compared to the point measurements. Furthermore, variability in observed dust amounts was not only caused by the patterns of dust deposition on the glacier, but also due to windblown transport over an undulating surface, or surface melt streams washing away surface dust. Such processes were not accounted for in the modelled dust patterns. Regarding the mean concentrations, at least part of the model high bias may, in fact, be due to a location bias in the measurements. Most of the measurement locations are in the accumulation zone of the glacier. Model grid cells containing the measurement locations often extend to the glacier edges, where deposition amounts are higher. Regardless of whether the model bias can be explained or not, the comparison shows that the order of magnitude of dust deposition on Vatnajökull is captured by the model.

Table 1 gives the measured and modelled dust deposition during the years 2012 and 2013 for stations on Brúarjökull, our main area of investigation. Again, the model tended to overestimate dust deposition.

3.2. Dust events on Brúarjökull 2012

FLEXPART results for both dust concentrations in the air and dust deposition on the glacier surface were reported for the dust events for the year 2012 at station B13 (Table 2) and B16 (Table 3). Albedo, temperature and wind at 2 m elevation were measured at the AWSs, while precipitation data were taken from the ECMWF model. At station B13 there were ten modelled dust events during the measuring period (9 May to 14 October 2012), and all of them were associated with an observed albedo drop during the event at the AWS. Four events had high dust concentrations and depositions (bold in Table 2), and six smaller events occurred as well (Figure 3). The highest deposition values were simulated during event 6 with 6.6 g m^{-2} of dust deposited during a period of 14 days with an albedo drop of 0.65 from the maximum to the minimum albedo value during that period. In contrast, at station B16 (Table 3) the largest deposition (5.2 g m^{-2}) occurred during event 1 with an albedo drop of 0.17. Two events, one occurred during sub-freezing temperatures, and the other during melting temperatures, were described in detail in section 3.2.1.

The albedo was almost always lower at site B13 than at site B16, due to the lower elevation and thus higher temperatures and increased melting at this site, and probably also because of its proximity to a major dust source area (Dyngjusandur). The biggest dust events happened in spring (mid-May) and autumn (end of August and October), especially at station B16. Dust event 5 coincided with warm summer temperatures and exposure of the ablation area, where albedo at B13 reached its lowest value, 0.08, on day 223. At the lower elevation site B13 (~1210 m a.s.l.), dust deposition and concentration values during dust events were always larger than at the higher site B16 (~1525 m a.s.l.), except for event 1 (section 3.2.1). The duration of the events was also often longer at B13 than at B16. Furthermore, no dust was simulated at station B16 during event 8 (Table 3).

3.2.1. Case studies

Two dust events have been chosen for a detailed description. Event no. 1 (Figure 4) was by far the biggest event at B16 and temperatures were below freezing all the time, and event no. 2 (Figure 5) happened, as was often the case, during melting temperatures. The analysis of event no. 2 was supported by the availability of a clear-sky MODIS image showing the dust cloud and deposition (Figure 6).

3.2.1.1. Dust event 1

Dust event 1 is one of four major modelled dust storms on Brúarjökull in 2012 (Figure 4) and the only event for which total simulated dust deposition was higher at station B16 (3.7 g m^{-2}) than at B13 (2.6 g m^{-2}). This explains why the albedo reached a lower value between day 134 and 139 at B16 than B13, which is very atypical. During the event, albedo dropped by 0.15 from 0.9 to 0.75 at B13 (Table 2) and by 0.17 from 0.88 to 0.72 at B16. Albedo peaked on day 133 at B16 and on day 134 at B13 because of snow fall. Simulated dust deposition started on day 134 at midday and lasted until day 136 (afternoon). This was the largest wet deposition event at both stations. At B13 (B16) there were 1.6 g m^{-2} (1.3 g m^{-2}) dust deposited as dry deposition and 2.1 g m^{-2} (3.9 g m^{-2}) as wet deposition, which at B16 was by far the largest deposition in a single event.

Near-surface dust concentration reached values of 193 μg m^{-3} at B13 and 121 μg m^{-3} at B16. Temperature decreased during the event and remained well below the freezing point, excluding the possibility that melt processes were responsible for the albedo drop. This strongly supports our hypothesis that the dust deposition caused the albedo reduction. Since dust was deposited during snowfall, the albedo drop is probably smaller than if the dust were deposited entirely by dry deposition. In fact, normally albedo increases during snowfall, so the dust deposition must have more than compensated this effect. Wind was blowing from the north during days 134-138, with high wind speeds on day 134 and 135 (B16 16 m s^{-1}, B13 11 m s^{-1}), indicating that dust was transported most likely from Dyngjusandur.

3.2.1.2.   Dust event 2

Dust event 2 is the second largest modelled dust event in terms of dust concentration and fourth biggest in terms of total deposition at station B13 (2.5 g m^{-2}) but it was much smaller at B16 (0.1 g m^{-2}) and started later (day 146). Dust concentrations at B13 (B16) reached 225 μg m^{-3} (19 μg m^{-3}). Dust deposition started in the afternoon on day 145 and albedo dropped on day 146 (from 0.73 to 0.60). During the whole dust event albedo dropped by 0.36 (from 0.86 to 0.5) at B13 and by 0.28 (from 0.87 to 0.59) at B16. Temperature rose above the freezing point on day 143 and this may partly explain the albedo reduction. However, the strongest albedo reduction coincided closely with the time period of the dust deposition. In particular, notice that the albedo did not decrease significantly after the end of the deposition event, even though temperatures (at least during daytime) remained above the freezing point.

Notice also that the albedo reduction was stronger at B13 than at B16, in agreement with the higher dust deposition at B13. Precipitation occurred until day 146, so mainly before dust deposition, suggesting that dust deposition was the main factor in this albedo drop. Wind was strongest on day 146 (13.6 m s^{-1} at B13) and from SW (glacier wind), but changed to WNW until day 149.

Figure 6 shows a comparison between two different MODIS images (before and after the dust event). It indicates the presence of the dust plume very clearly during event 2 over the glacier, as the brownish hues are normally not present there.

3.2.2. Average dust event at B13 in 2012

330   Using the values reported in Table 2, we calculated averages to characterize an *average* dust event at the B13 site. On average a dust event at station B13 in 2012 lasted for 6 days, had a maximum dust concentration of 122 µg m^{-3} and a total deposition of 2 g m^{-2}. Dry deposition in all cases except the first event exceeded wet deposition. This is due to the proximity of the measurement site to the source area and gravitational settling of larger particles, which dominated the removal near the

335   source. The albedo is on average lowered by 0.18 in a dust event. This large reduction had a strong impact on the radiation and energy balance of the glacier. The average temperature during dust events was -2°C (at ~1210 m elevation) and the prevailing wind direction in 80% of the events was northerly, in 20% it is SW (the direction of the glacier wind on Brúarjökull). Average ECMWF precipitation during events was ~23 mm.

340   ### 3.3. Surface energy balance impact of dust deposition

Deposition of dark dust particles on a glacier surface lowers the surface albedo, thus also the surface energy balance and in general increases the energy available for melt. In order to estimate the contribution of this effect, the surface energy balance (and the surface melt from energy balance) at the two AWS sites B13 and B16 was estimated from the AWS data in 2012. To estimate the effect,

345   the regional climate model HIRHAM5 was used to simulate a clean glacier surface for the weather conditions occurring at the AWS B13 and B16 in 2012. The simulated clean surface albedo (black line in Figure 7) is compared to the observed albedo including impurities (red line in Figure 7). Generally, the model captures the measured albedo variability; however, the observed albedo is more variable and reaches lower values between events of snowfall. Since this is a simple model, we are not

350   expecting the model to capture all details. The statistical fit for HIRHAM5 compared to the AWS data showed a better fit for years with higher albedos where the previous summer surface did not melt out. The average bias, taken as the difference between HIRHAM5 and AWS data, is 0.08 for the years 1997-2014 whereas for the year 2012 it is 0.18 which means an overestimate by the model. The correlation coefficient for measured and simulated albedo data for the year 2012 is 0.77, which is

355   higher than the average value for other years of 0.68.

The difference between the modelled clean surface and the real surface is greater at B13 than B16. This was expected since dust concentration is much higher at the lower site B13 and snowfall more common at the upper site B16. We also know from mass balance measurements, that at B13 all the

winter snow melted, exposing firn and surface dust from previous years (this happened at day ~205).

360 With addition of dust from dust events starting on days 202 and 220 (Figure 8) the albedo values dropped very low at B13 between days 220 and 236. The simulated energy balance did not predict the snow from the previous winter to have been melted away completely, exposing the firn layer.

High temperatures at B13 up to ~5 °C coincide with dust event 5, which caused peaks in snow melt of 8.13 cm w.e. d^{-1} on day 222. In the autumn, after day ~240, the energy balance was mostly negative.

365 Low net radiation is caused by low solar radiation due to shorter days and high albedo caused by snow fall. This is accompanied with negative turbulent heat fluxes (due to air temperatures below zero and strong winds) and resulted in negative total energy, i.e. no energy available for melting in 2012.

The total summer melt at B13 in 2012 estimated from the energy balance calculated for a dust free

370 surface was 1.7 m w.e., whereas for the measured albedo the melt was estimated at 2.8 m w.e. From this we conclude that the melt increased by 1.1 m w.e., or by ~60%, due to dust deposition, and melting out of the dusty firn surface below. Other impurities such as black carbon were expected to be negligible (Dadic et al., 2013, Fig. 12a; Meinander et al., 2014). At the higher site, B16, 1.0 m w.e. of snow melt was calculated for the modelled dust free surface and 1.6 m w.e. when using the

375 measured albedo, which results in 0.6 m more snow melt caused by dust on the surface. The increase in melt is similar to that in B13, i.e. additional 60%.

4. Discussion and conclusions

In this paper, we have shown that dust events modelled by FLEXDUST correspond to reductions in the observed albedo at two AWS sites on Vatnajökull. This indicates that the model is able to capture

380 the occurrence of individual dust events. Furthermore, we showed that the model captures both the observed spatial distribution of dust on the glacier as well as the order of magnitude of the total annual deposition amounts. This suggests that the model can be used for longer-term studies, to quantify the dust deposition on Vatnajökull, including its interannual variability. Table 2 shows the dust events of the year 2012 at station B13 on Brúarjökull, where in total 10 dust events occurred;

385 four main events and six smaller events. The AWS measurements show a drop in albedo in connection to all dust events predicted by FLEXPART within the AWS's survey period. The prevailing wind direction during dust events at site B13 is from a northerly direction, while for the whole period downslope (SW) winds dominate. The wind direction during dust events corresponds to the main dust source Dyngjusandur, north of Vatnajökull. At site B16, situated further upglacier, 9 dust events

390 occurred (Table 3) where the first dust event with ~5 g m^{-2} of dust deposited within 3 days was by far the largest.

In Arnalds et al. (2014) average deposition of dust on Icelandic glaciers is estimated as ~400 g m^{-2} yr^{-1} which seems to be an overestimate in the light of results presented here. Their estimate includes periodic tephra deposition and large dust events based on a country average and it does not adequately account for topographic differences and that much of the glacial areas are upwind for dry winds from the main dust sources at the glacial margins. With FLEXPART, we calculated much lower annual deposition rates for Vatnajökull and its surroundings in 2013 (Figure 2), up to 34 g m^{-2} in the SW of the glacier. Moreover, modelled values for dust deposition rates on Brúarjökull of 20 g m^{-2} (B13) and 10 g m^{-2} (B16) for 2012 were much lower.

Firn core B drilled on Brúarjökull showed a dust layer of ~8 g m^{-2} for 2012 (Table 1), in very good agreement with the simulated dust of 8.5 g m^{-2}. At firn core (A), drilled in the immediate vicinity of core B, observed deposition rate was much smaller (1.7 g m^{-2}), showing the large spatial variability and consequent uncertainty in comparing point measurements to model simulations. We thus consider the model results satisfactory if they are in the same order of magnitude as observed dust amounts in ice cores or snow samples.

To estimate the impact of dust on the surface energy balance and melt rates, the regional climate model HIRHAM5 was used to simulate the surface albedo for a dust free, i.e. clean snow surface during the summer 2012. The surface energy balance (and melt rate) was calculated using the simulated albedo and the albedo observed from the AWS data. At the lower site, B13, the difference between dust free and real surface is 1.1 m w.e. of more snow melt (1.7 m w.e. snow melt for the clean surface and 2.8 m w.e. for the real surface). This does not only include dust events lowering surface albedo, but also dust and tephra that was deposited during previous years melting out from below. At the upper site B16 the difference results in 0.6 m of more snow melt (1.0 m w.e. for the clean surface and 1.6 m w.e. for the AWS). Since B16 is situated in the accumulation area, no dust expected to melt out from below. It cannot be excluded that small amounts of organic material or black carbon are deposited on the snow surface and influence albedo, but from in situ investigations this has not been observed in this area.

The year 2012 was a year of intensive summer melt. At site B13 on Vatnajökull the measured summer mass balance was 2.3 m w.e. mass loss, which means 0.5 m more mass loss than the average since 1993 (1.7 m w.e.). Summer mass balance measurements on Vatnajökull show 2.3 m w.e. of total mass loss at B13 which is 0.5 m less melt compared to calculated energy balance converted into snow melt (2.8 m w.e.). Most of these differences is assigned to summer snow fall that melts, and was not captured with the mass balance measurements.

Oerlemans et al. (2009) reported that decreased albedo at Vadret da Morteratsch glacier caused an additional removal of about 3.5 m of ice for the 4 year period 2003–06. This means 0.9 m more melt on average per year. Gabbi et al. (2015) compared a glacier surface with deposits of black carbon and Saharan dust to pure snow conditions for a 100 year period (1914-2014). They found that the mean annual albedo decreased by 0.04–0.06, therefore the mean annual mass balance was reduced by about 28–49 cm. These alpine melt rates due to impurities are in the same order of magnitude as our results.

Albedo comparisons for other years (Appendix, Fig. A3) have shown very low albedo values for the years 1997, 2004, 2005 and 2012. The surface dirt causing the low albedo in 1997 is related to the Gjálp eruption in 1996, and the following huge jökulhlaup with deposition of fine grained particles on Skeiðarársandur sandur plain. This was a vast source of dust in the dry and warm 1997 summer. The low albedo in 2005 and 2012 most likely also related to the 2004 and 2011 Grímsvötn eruptions (e.g. Guðmundsson et al. 2004, Möller et al. 2013.) In 2004 increased melt rates due to high wind-driven turbulent heat fluxes in the end of July followed by exceptionally warm and sunny weather in August sped up melting into old firn (Guðmundsson et al. 2006).

The results in this paper shows positive radiative forcing impact on snow melt of Icelandic glaciers caused by deposition of dust that strongly enhances absorption of light. The duration of dust radiative effects on glacier surfaces is extended compared to purely atmospheric effects because of the short lifetime of dust in the atmosphere.

Acknowledgements

The study described in this manuscript was supported by NordForsk as part of the two Nordic Centres' of Excellence Cryosphere-atmosphere interactions in a changing Arctic climate (CRAICC), and eScience Tools for Investigating Climate Change (eSTICC). Part of this work was supported by the Centre of Excellence in Atmospheric Science funded by the Finnish Academy of Sciences Excellence (project no. 272041), by the Finnish Academy of Sciences project A4 (contract 254195). Data from in situ mass balance surveys and on glacier automatic weather stations is from joint projects of the National Power Company and the Glaciology group of the Institute of Earth Science, University of Iceland. C. Groot Zwaaftink was also funded by the Swiss National Science Foundation SNF (155294), and Louise Steffensen-Schmidt, Finnur Pálsson and Sverrir Guðmundsson by the Icelandic Research Fund (project SAMAR) and the National Power Company of Iceland. Ólafur Arnalds was in part funded by Icelandic Research Fund (grant no. 152248-051)

5. References:

AMAP Assessment 2015: Black carbon and ozone as Arctic climate forcers. Arctic Monitoring and Assessment Programme (AMAP), Oslo, Norway. vii + 116 pp, 2015.

460 Arnalds, O., Olafsson, H., Dagsson-Waldhauserova, P.: Quantification of ironrich volcanogenic dust emissions and deposition over ocean from Icelandic dust sources. Biogeosciences 11, 6623–6632. http://dx.doi.org/10.5194/bg-11-6623-, 2014.

Arnalds, O.: The soils of Iceland, 160 pp., Springer, Dordrecht, The Netherlands, 2015.

Arnalds, O., Dagsson-Waldhauserova, P., & Olafsson, H.: The Icelandic volcanic aeolian environment: 465 Processes and impacts—A review. Aeolian Research, 20, 176-195; 2016.

Arnalds, O., Gisladottir, F.O., Sigurjonsson, H: Sandy deserts of Iceland: an overview. Journal of Arid Environments 47, 359–371, 2001.

Baddock, M. C., Mockford, T., Bullard, J. E., & Thorsteinsson, T.: Pathways of high-latitude dust in the North Atlantic. Earth and Planetary Science Letters, 459, 170-182, 2017.

470 Benn, D. and Evans, D. J.: Glaciers and glaciation. Second edition. 802 pp. Routledge, 2010.

Björnsson, H., & Pálsson, F.: Icelandic glaciers. Jökull, 58, 365-386, 2008.

Björnsson, H., Pálsson, F., Gudmundsson, S., Magnússon, E., Adalgeirsdóttir, G., Jóhannesson, T., Berthier, E., Sigurdsson, O.,and Thorsteinsson, Th.: Contribution of Icelandic ice caps to sea level rise: Trends and variability since the Little Ice Age. Geophysical Research Letters, Vol. 40, 1-5, 475 doi:10.1002/grl.50278, 2013.

Budyko, M. I.: The effect of solar radiation variations on the climate of the earth. Tellus, 21(5), 611-619, 1969.

Cuffey, K. M., & Paterson, W. S. B.: The physics of glaciers, 693pp, Academic Press, 2010.

Dadic, R., Mullen, P. C., Schneebeli, M., Brandt, R. E., & Warren, S. G. Effects of bubbles, cracks, and 480 volcanic tephra on the spectral albedo of bare ice near the Transantarctic Mountains: Implications for sea glaciers on Snowball Earth. Journal of Geophysical Research: Earth Surface, 118(3), 1658-1676, 2013.

Dagsson-Waldhauserova, P., Arnalds, O., & Olafsson, H.: Long-term frequency and characteristics of dust storm events in Northeast Iceland (1949–2011). Atmospheric Environment, 77, 117-127, 2013.

485   Dagsson-Waldhauserova, P., Arnalds, O., Olafsson, H., Skrabalova, L., Sigurdardottir, G. M., Branis, M., et al.: Physical properties of suspended dust during moist and low wind conditions in Iceland. Icelandic Agricultural Sciences, 27, 25-39, 2014.

Dagsson-Waldhauserova, P., Arnalds, O., Olafsson, H., Hladil, J., Skala, R., Navratil, T., ... & Meinander, O.: Snow–dust storm: unique case study from Iceland, March 6–7, 2013. Aeolian
490   Research, 16, 69-74, 2015.

Davies, S. M., Larsen, G., Wastegård, S., Turney, C. S., Hall, V. A., Coyle, L., & Thordarson, T.: Widespread dispersal of Icelandic tephra: how does the Eyjafjöll eruption of 2010 compare to past Icelandic events?. Journal of Quaternary Science, 25(5), 605-611, 2010.

Di Mauro, B., Fava, F., Ferrero, L., Garzonio, R., Baccolo, G., Delmonte, B., & Colombo, R.: Mineral
495   dust impact on snow radiative properties in the European Alps combining ground, UAV, and satellite observations. Journal of Geophysical Research: Atmospheres, 120(12), 6080-6097, 2015

Doherty, S. J., Grenfell, T. C., Forsström, S., Hegg, D. L., Brandt, R. E., & Warren, S. G.: Observed vertical redistribution of black carbon and other insoluble light-absorbing particles in melting snow. Journal of Geophysical Research: Atmospheres, 118(11), 5553-5569, 2013.

500   Dragosics, M., Meinander, O., Jónsdóttir, T., Dürig, T., De Leeuw, G., Pálsson, F., Dagsson-Waldhauserová, P., and Thorsteinsson, Th.: Insulation effects of Icelandic dust and volcanic ash on snow and ice. Arab. J. Geosci., 9, 126, 2016.

Eerola, K.: About the performance of HIRLAM version 7.0. HIRLAM Newsletter, 51:93–102, 2006.

Flanner, M. G., Zender, C. S., Randerson, J. T., & Rasch, P. J.: Present-day climate forcing and
505   response from black carbon in snow. Journal of Geophysical Research: Atmospheres, 112(D11), 2007.

Flanner, M. G., Gardner, A. S., Eckhardt, S., Stohl, A., and Perket, J.: Aerosol radiative forcing from the 2010 Eyjafjallajökull volcanic eruptions. J. Geophys. Res. 119, 9481-9491, doi:10.1002/2014JD021977, 2014.

Gabbi, J., Huss, M., Bauder, A., Cao, F., & Schwikowski, M.: The impact of Saharan dust and black
510   carbon on albedo and long-term mass balance of an Alpine glacier. The Cryosphere, 9(4), 1385-1400, 2015.

Gölles, T., Bøggild, C. E., & Greve, R.: Ice sheet mass loss caused by dust and black carbon accumulation. The Cryosphere, 9(5), 1845-1856, 2015. doi:10.5194/tc-9-1845-2015

Greuell, W., Genthon, C.: Mass Balance of the Cryosphere: Observations and Modelling of

515   Contemporary and Future Changes, eds. Jonathan L. Bamber and Antony J. Payne. Published by Cambridge University Press. Cambridge University Press, 2003.

Groot Zwaaftink, C. D., Grythe, H., Skov, H. and Stohl, A.: Substantial contribution of northern high-latitude sources to mineral dust in the Arctic, J. Geophys. Res. Atmos., 121, doi:10.1002/2016JD025482, 2016

520   Guðmundsson, S., Björnsson, H., Pálsson, F. and Haraldsson, H. H.: Energy balance of Brúarjökull and circumstances leading to the August 2004 floods in the river Jökla, N-Vatnajökull (Vol. 55, pp. 1-18). Jökull, 2006.

Guðmundsson, S., Björnsson, H., Pálsson, F., & Haraldsson, H. H.: Comparison of energy balance and degree-day models of summer ablation on the Langjökull ice cap, SW-Iceland. Jökull, 59, 1-18, 2009.

525   Hansen, J., & Nazarenko, L.: Soot climate forcing via snow and ice albedos. Proceedings of the National Academy of Sciences of the United States of America, 101(2), 423-428, 2004.

He, C., Li, Q. B., Liou, K. N., Takano, Y., Gu, Y., Qi, L., Mao, Y. H., and Leung, L. R.: Black carbon radiative forcing over the Tibetan Plateau, Geophys. Res. Lett., 41, 7806-7813, doi:10.1002/2014gl062191, 2014.

530   Hock, R.: Glacier melt: a review of processes and their modelling. Progress in physical geography, 29(3), 362-391, 2005.

IPCC: Climate change 2013: The physical science basis. In: Working Group I, Contribution to the IPCC 5th Assessment Report – summary for policy makers, 2013.

Kipp&Zonen Instruction Manual for Pyranometer/Albedometer CM11 and CM14.

535   http://www.kippzonen.com, 2000, accessed August 2016.

Kok, J. F.: A scaling theory for the size distribution of emitted dust aerosols suggests climate models underestimate the size of the global dust cycle. Proceedings of the National Academy of Sciences, 108(3), 1016-1021, 2011.

Langen, P. L., Mottram, R. H., Christensen, J. H., Boberg, F., Rodehacke, C. B., Stendel, M., van As, D.,

540   Ahlstrøm, A.P., Mortensen, J., Rysgaard, S., Petersen, D., Svendsen, K. H. , Aðalgeirsdóttir, G. and Cappelen J.: Quantifying Energy and Mass Fluxes Controlling Godthåbsfjord Freshwater Input in a 5-km Simulation (1991–2012). Journal of Climate, 28(9), 3694-3713, 2015.

Lucas-Picher, P., Wulff-Nielsen, M., Christensen, J. H., Adalgeirsdóttir, G., Mottram, R. H. and Simonsen, S. B.: Very high resolution regional climate model simulations over Greenland: Identifying added value. Journal of Geophysical Research, 117:2108, 2012.

Marticorena, B. and Bergametti, G.: Modeling the atmospheric dust cycle: 1. Design of a soil-derived dust emission scheme. Journal of Geophysical Research: Atmospheres, 100(D8), 16415-16430, 1995.

Meinander, O., Kontu, A., Virkkula, A., Arola, A., Backman, L., Dagsson-Waldhauserová, P., ... & Leppäranta, M. Brief communication: Light-absorbing impurities can reduce the density of melting snow. The Cryosphere, 8(3), 991-995, 2014.

Meinander, O., Dagsson-Waldhauserova, P. and Arnalds, O.: Icelandic volcanic dust can have a significant influence on the cryosphere in Greenland and elsewhere. Polar Research, 35, 2016.

Möller, R., Möller, M., Björnsson, H., Guðmundsson, s., Pálsson, F., Oddsson, B., Kukla, P. A., Schneider, C.: MODIS-derived albedo changes of Vatnajökull (Iceland) due to tephradeposition from the 2004 Grímsvötn eruption. International Journal of Applied Earth Observation and Geoinformation 26, 256-269, 2013.

Myhre, G., Shindell, D., Bréon, F. M., Collins, W., Fuglestvedt, J., Huang, J., ... & Nakajima, T.: Anthropogenic and Natural Radiative Forcing. In: Climate Change 2013: The Physical Science Basis. Contribution of Working Group 1 to the Fifth Assessment Report of the Intergovernmental Panel on Climate Change. Table, 8, 714, 2013.

Nielsen-Englyst, P.: Impact of albedo parameterizations on surface mass balance and runoff on the Greenland Ice Sheet. Master's thesis University of Copenhagen, unpublished, 2015.

Oerlemans, J., & Knap, W. H.: A 1 year record of global radiation and albedo in the ablation zone of Morteratschgletscher, Switzerland. *Journal of Glaciology*, *44*(147), 231-238, 1998.

Oerlemans, J.: *Glaciers and climate change*. CRC Press, 2001.

Oerlemans, J., Giesen, R. H., & Van den Broeke, M. R.: Retreating alpine glaciers: increased melt rates due to accumulation of dust (Vadret da Morteratsch, Switzerland). Journal of Glaciology, 55(192), 729-736, 2009.

Painter, T. H., A. P. Barrett, C. C. Landry, J. C. Neff, M. P. Cassidy, C. R. Lawrence, K. E. McBride, and G. L. Farmer: Impact of disturbed desert soils on duration of mountain snow cover, Geophys. Res. Lett., 34, L12 502, doi:10.1029/2007GL030284, 2007.

Painter, T. H., Flanner, M. G., Kaser, G., Marzeion, B., VanCuren, R. A., & Abdalati, W.: End of the Little Ice Age in the Alps forced by industrial black carbon. Proceedings of the national academy of sciences, 110(38), 15216-15221, 2013.

575   Petit, J. R., Wegner, A., Narsici, B., Svensson, A., Bigler, M., & Steffensen, J. P.: The NEEM record of aeolian dust: contributions from Coulter counter measurements. In EGU General Assembly Conference Abstracts (Vol. 15, p. 6255), 2013.

Quinn, P. K., Bates, T. S., Baum, E., Doubleday, N., Fiore, A. M., Flanner, M., ... & Shindell, D.: Short-lived pollutants in the Arctic: their climate impact and possible mitigation strategies. Atmospheric
580   Chemistry and Physics, 8(6), 1723-1735, 2008.

Roeckner, E., Bäuml, G., Bonaventura,L., Brokopf, R., Esch, M.,Giorgetta, M., Hagemann, S., Kirchner, I.,Kornblueh, L., Manzini, E., Rhodin, A., Schlese, U., Schulzweida, U. and Tompkins , A.: The atmospheric general circulation model ECHAM 5 PART I: Model description. Technical Report 349, Report / MPI für Meteorologie, 2003.

585   Schmidt, L. S., Aðalgeirsdóttir, G., Guðmundsson, S., Langen, P. L., Pálsson, F., Mottram, R., Gascoin, S., and Björnsson, H.: The importance of accurate glacier albedo for estimates of surface mass balance on Vatnajökull: Evaluating the surface energy budget in a Regional Climate Model with automatic weather station observations, The Cryosphere Discuss., doi:10.5194/tc-2017-14, in review, 2017.

590   Stohl, A., Hittenberger, M., and Wotawa, G.: Validation of the Lagrangian particle dispersion model FLEXPART against large-scale tracer experiment data. Atmospheric Environment, 32(24), 4245-4264, 1998.

Stohl, A., Forster, C., Frank, A., Seibert, P., and Wotawa, G.: Technical Note : The Lagrangian particle dispersion model FLEXPART version 6.2. Atmos. Chem. Phys. 5, 2461-2474, 2005.

595   Wiscombe, W. J., & Warren, S. G.: A model for the spectral albedo of snow. I: Pure snow. Journal of the Atmospheric Sciences, 37(12), 2712-2733, 1980.

Yoshida, A., Moteki, N., Ohata, S., Mori, T., Tada, R., Dagsson-Waldhauserová, P., & Kondo, Y.: Detection of light-absorbing iron oxide particles using a modified single-particle soot photometer. Aerosol Science and Technology, 50(3), 1-4. DOI: 10.1080/02786826.2016.1146402, 2016.

600   Zhao, C., Hu, Z., Qian, Y., Ruby Leung, L., Huang, J., Huang, M., ... & Yan, H.: Simulating black carbon and dust and their radiative forcing in seasonal snow: a case study over North China with field campaign measurements. Atmospheric Chemistry and Physics, 14(20), 11475-11491, 2014.
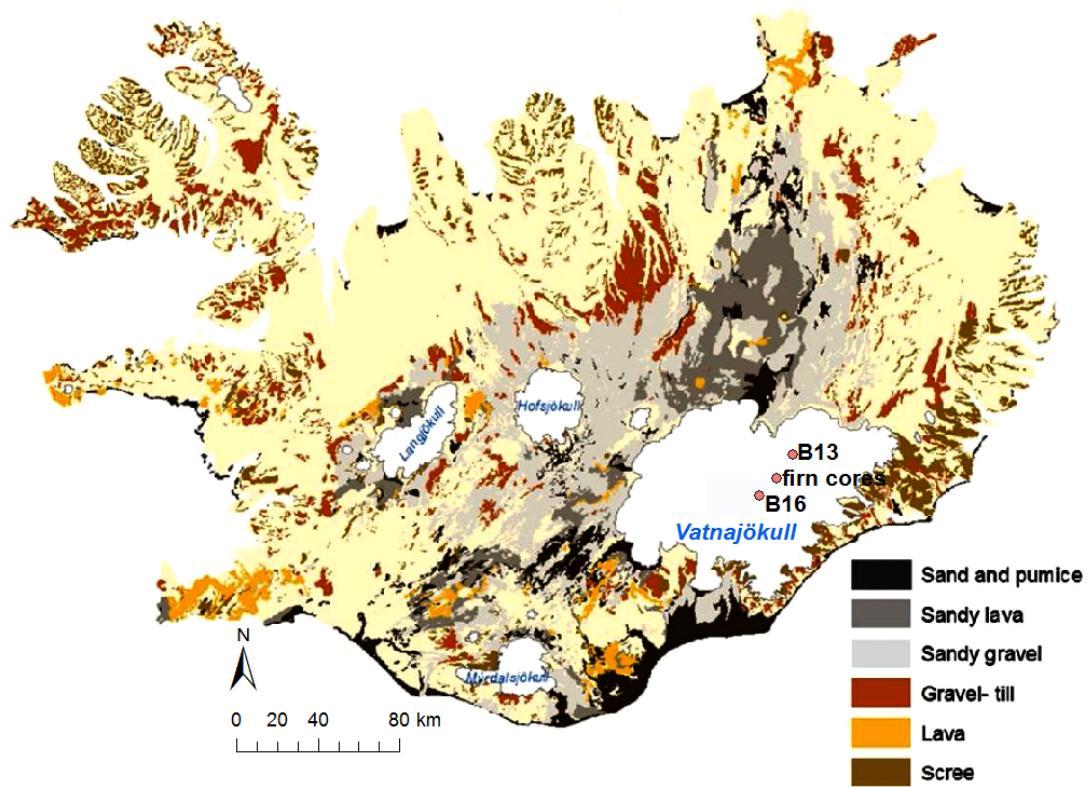
605 *Figure 1. Iceland with glacier outlines and soil map adapted from Arnalds (2015). The two AWSs at B13 and B16 as well as the firn core drill site on Brúarjökull are highlighted*
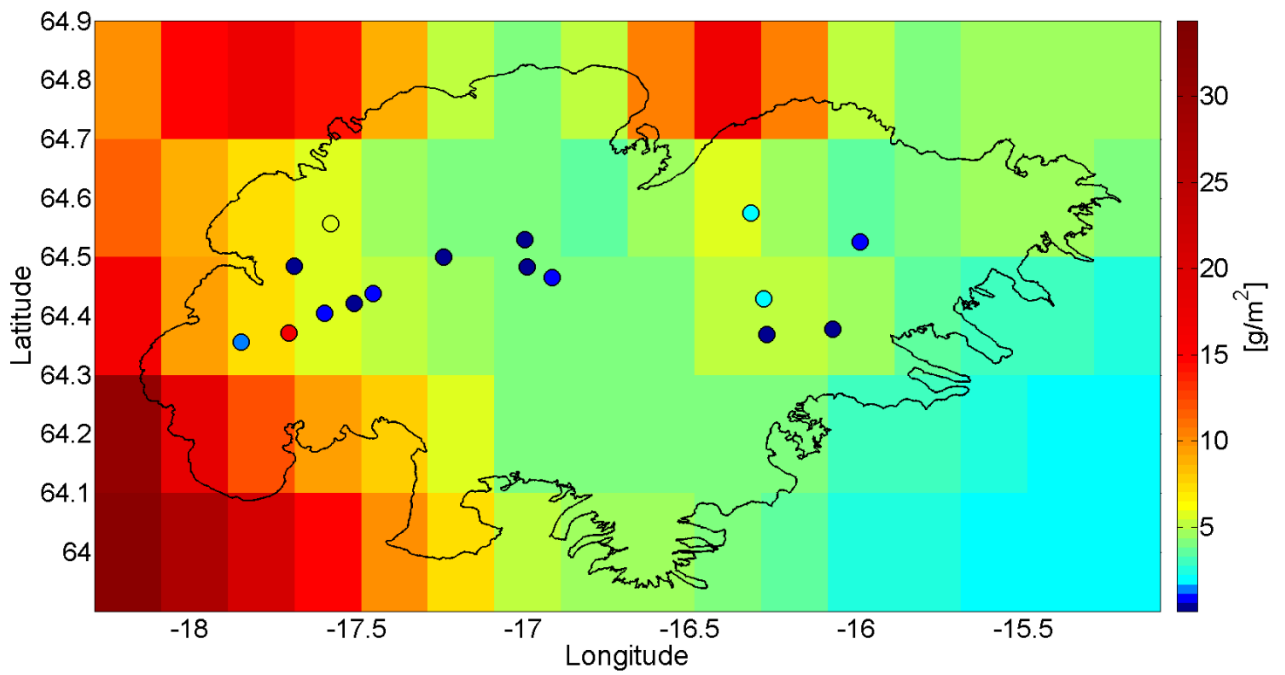
Figure 2: FLEXPART model simulation of the spatial dust distribution on Vatnajökull from January 1 until October 7 2013, the day when the surface snow samples have been taken. The circles show the location of snow sample sites with dust deposition for the same year.
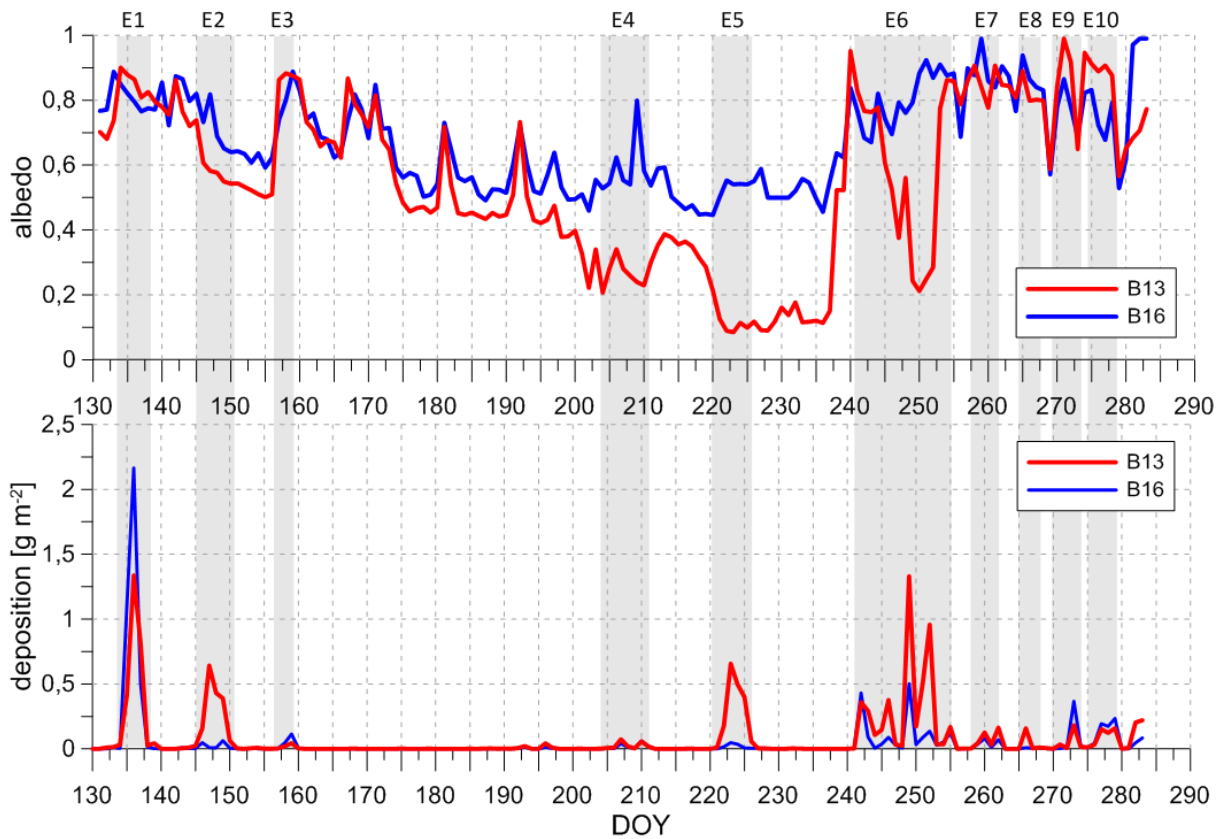
Figure 3: Upper graph: Albedo measurement from the AWS at B13 in red and B16 in blue for the measurement period in 2012. Lower graph: Daily dust deposition showing dust events modelled by FLEXPART. Dust events are highlighted in grey and named E1-E10.
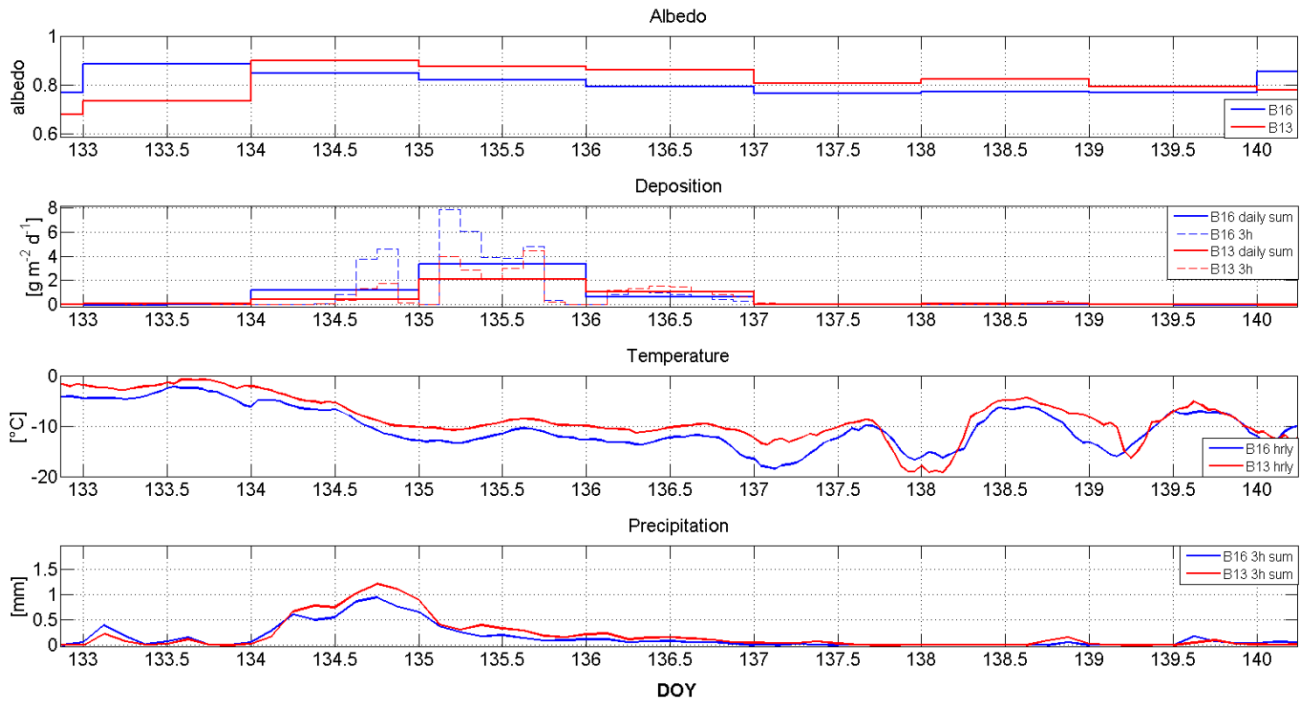
Figure 4: Observed albedo, simulated dust deposition, observed temperature and simulated precipitation dust event no. 1 at stations B16 (blue) and B13 (red). Modelled deposition is shown for 3-hourly and daily averages.
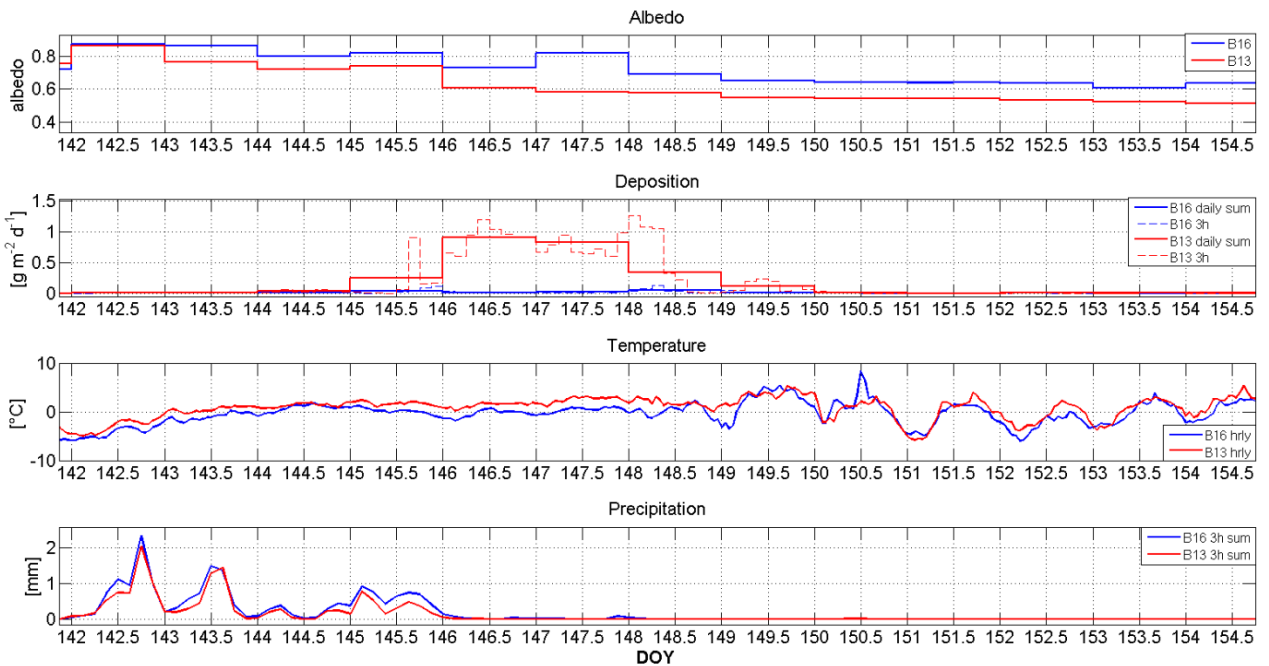
620 *Figure 5: Observed albedo, simulated dust deposition, observed temperature and simulated precipitation dust event no. 2 at stations B16 (blue) and B13 (red). Modelled deposition is shown for 3-hourly and daily averages.*
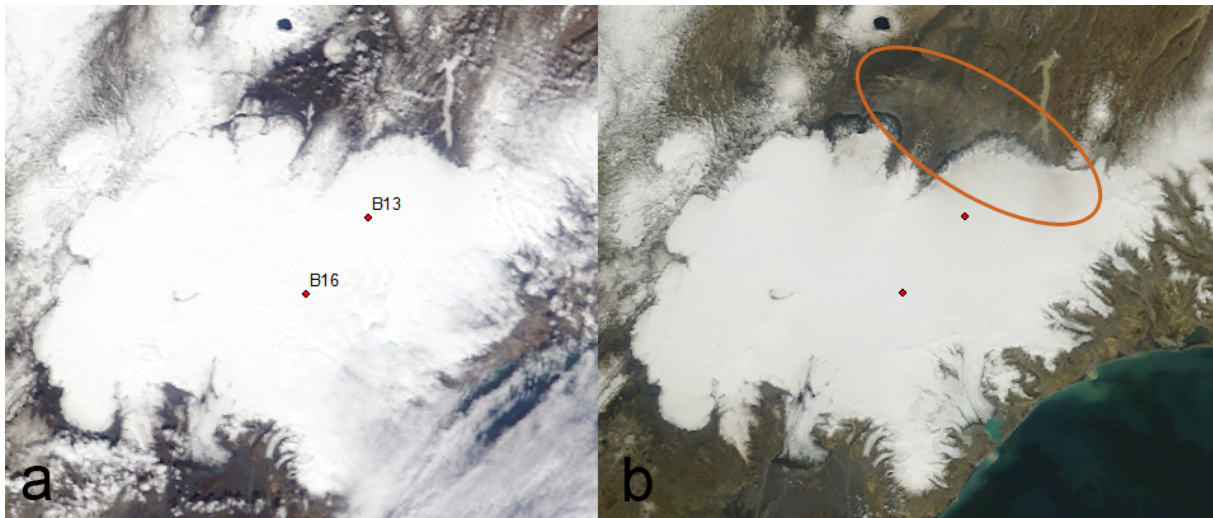
625 *Figure 6: MODIS images of Iceland on a) 20 May 2012 (day 141) and b) 28 May 2012 (day 149). Notice the brownish hues (orange circle) on Brúarjökull outlet (north-Vatnajökull) after the dust event, which indicate that dust was deposited on the glacier. Image courtesy of MODIS Rapid Response System at NASA/GSFC. http://rapidfire.sci.gsfc.nasa.gov/*
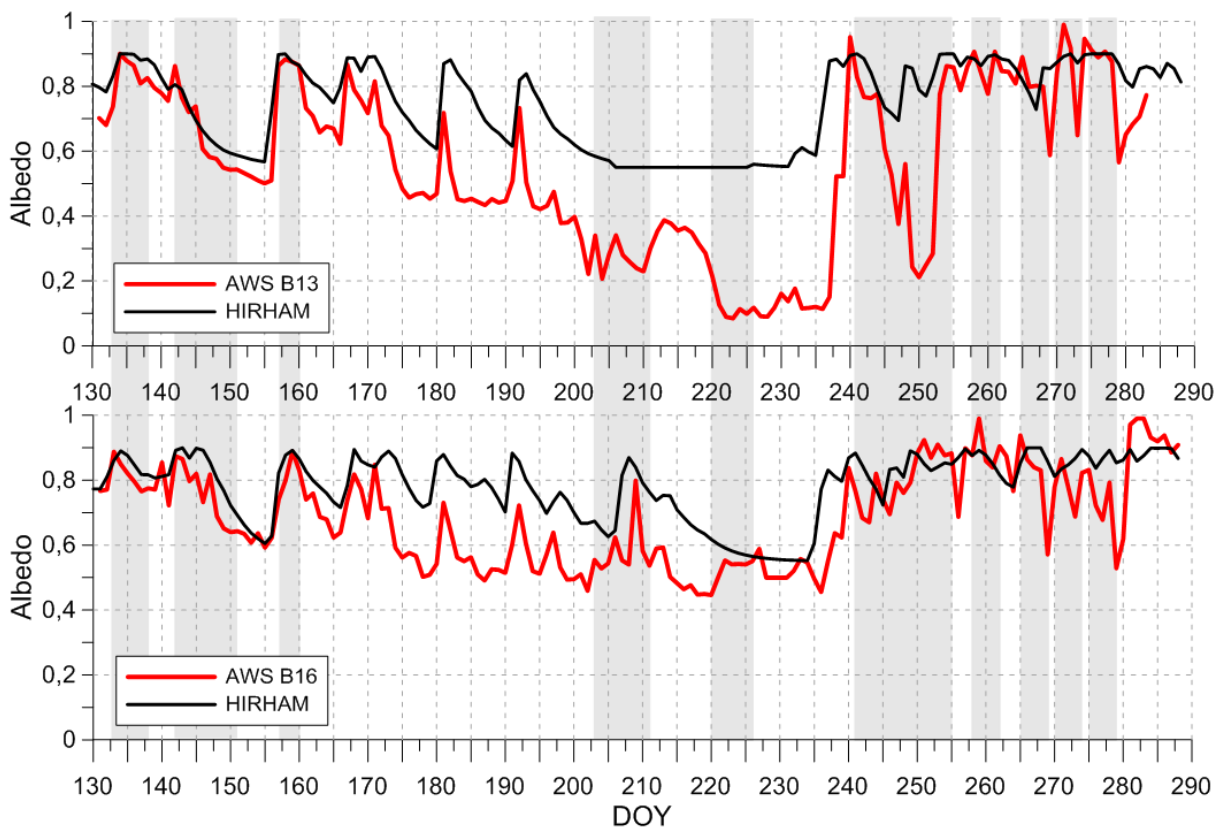
630 *Figure 7: Measured albedo (red line) and albedo simulated with HIRHAM5 (black line) for a clean glacier surface without dust at the stations B13 (upper graph) and B16 (lower graph). Highlighted in grey are modelled dust event periods by FLEXPART.*
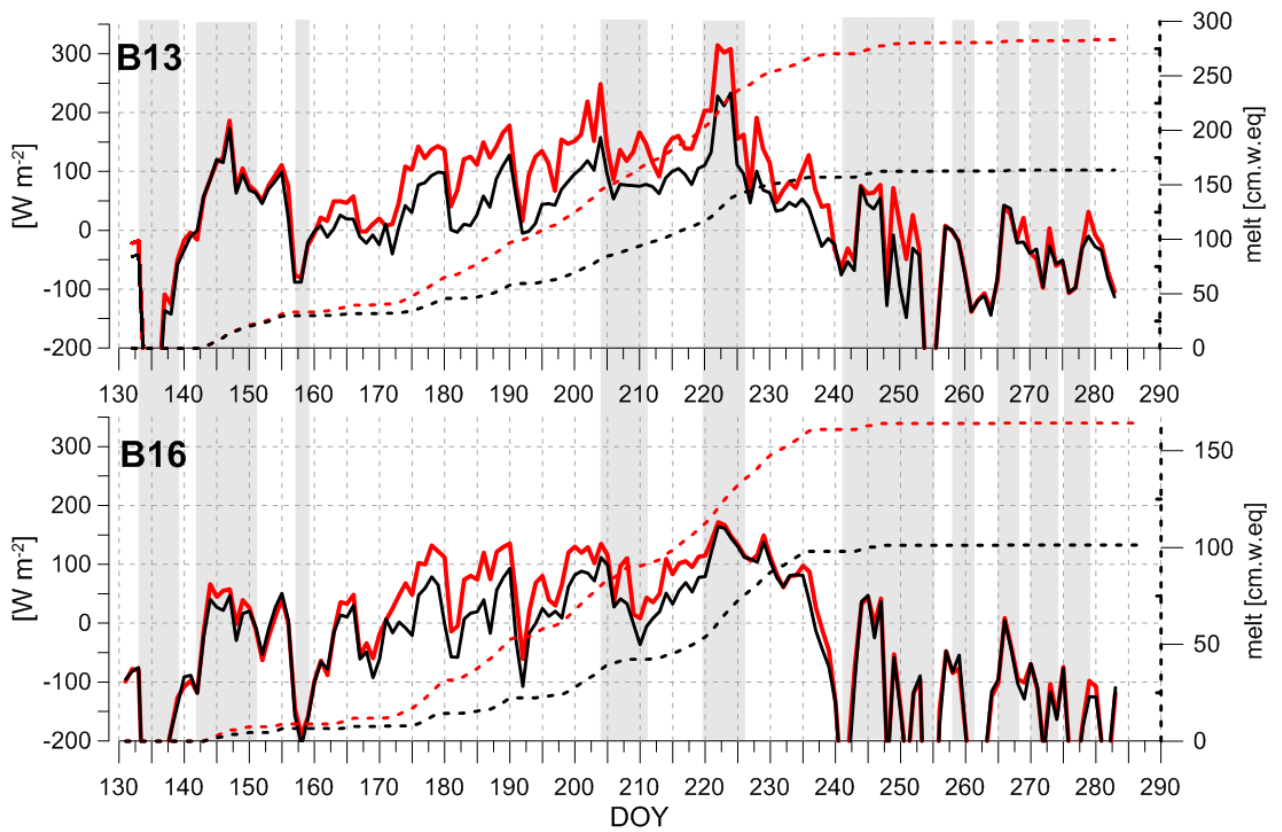
635   *Figure 8: Measured energy balance (red line) and energy balance with simulated albedo with HIRHAM5 (black line) for a clean glacier surface without dust at the stations B13 (upper graph) and B16 (lower graph). Cumulative snow melt is shown in dotted lines for AWS in red and HIRHAM5 in black. Highlighted in grey are modelled dust event periods by FLEXPART.*

Table 1: Total dust deposition [g m^{-2}] at stations on Brúarjökull in 2012 and 2013. Drill site A (Figure 1) is situated at station B15, drill site B 600 m below B15 at 1400 m elevation.

2012	Measurements	Model
B16		10.4
B13		20.5
firn core 2015 A	1.7	9.1
firn core 2015 B	7.9	8.5
2013		
B13	2.0	9.4

Table 2: Dust events at station B13. Reported are the modelled maximum and minimum dust concentration, the maximum simulated daily deposition as well as the total deposition during the event, the measured albedo change, maximum and minimum temperature and wind direction from the AWS, and the precipitation sum from the ECMWF model.

Event Nr.	DOY	Duration [days]	Concentration [$\mu g m^{-3}$]	Deposition [$g m^{-2}$]		Albedo change		Temperature [°C]		Wind	Precipitation ECMWF [mm]
			max	max	sum	max-min	start-end	min	max	main direction	sum
1	**133-138**	6	192,84	2,09	**3,70**	0,15	0,15	-12,7	-4,8	N	31
2	**142-150**	9	225,12	0,90	**2,48**	**0,36**	0,36	-2,9	3,4	E,S to NW	24
3	157-158	2	13,75	0,06	0,09	0,26	0,26	-3,8	-0,3	NNE	11
4	204-210	7	49,38	0,10	0,23	0,13	0,11	-0,1	2,4	S to N	19
5	**220-225**	6	212,07	1,02	**2,68**	0,04	0,04	2,0	4,8	SW	0
6	**241-254**	14	298,29	1,77	**6,60**	**0,65**	0,09	-6,2	2,4	SW to N,SE	114
7	258-261	4	44,89	0,19	0,37	0,13	0,13	-4,9	-2,4	NW to N	14
8	265-267	3	49,87	0,21	0,23	0,30	0,30	-5,1	1,4	SW,SE	48
9	270-272	3	67,86	0,29	0,33	0,34	0,34	-4,0	-1,8	W,NE,N	32
10	275-278	4	67,34	0,22	0,64	0,35	**0,35**	-10,3	-2,5	NNE	29

Table 3: Same as Table 2 but for station B16.

Event Nr.	DOY	Duration [days]	Model Concentration[μgm^{-3}] max	Model Deposition [gm^{-2}] max	Model Deposition [gm^{-2}] sum	AWS Albedo change max-min	AWS Albedo change start-end	AWS Temperature [°C] min	AWS Temperature [°C] max	AWS Wind main direction	Precipitation ECMWF [mm] sum
1	**134-136**	3	120,96	3,36	**5,22**	0,17	0,17	-14,3	-6,0	N	25
2	**145-149**	6	19,39	0,05	**0,12**	**0,28**	0,28	-4,1	2,5	once around clockwise	2
3	157-158	2	15,33	0,12	**0,17**	**0,27**	0,27	-5,1	-0,3	NNE	16
4	206-210	5	21,14	0,06	0,15	0,26	0,04	2,5	7,6	N,SW,N	4
5	221-223	3	15,01	0,07	0,15	0,01	0,01	2,2	2,9	SW	2
6	**241-254**	14	71,44	0,66	**2,34**	**0,25**	-0,04	-8,4	0,7	N,SW	110
7	258-259	2	27,92	0,07	**0,10**	0,13	0,13	-6,8	-3,7	W	4
8	no event										
9	270-273	3	51,31	0,53	0,55	0,18	0,18	-5,4	-4,7	SW,E,N	22
10	**275-278**	4	45,27	0,22	**0,64**	**0,30**	0,30	-8,7	-4,2	N	14

650